

Evaluating Transformer-based Semantic Segmentation Networks for Pathological Image Segmentation

Cam Nguyen^a, Zuhayr Asad^a, and Yuankai Huo^a

^aDepartment of Computer Science, Vanderbilt University, Nashville, TN, 37235 USA

ABSTRACT

Histopathology has played an essential role in cancer diagnosis. With the rapid advances in convolutional neural networks (CNN). Various CNN-based automated pathological image segmentation approaches have been developed in computer-assisted pathological image analysis. In the past few years, Transformer neural networks (Transformer) have shown the unique merit of capturing the global long-distance dependencies across the entire image as a new deep learning paradigm. Such merit is appealing for exploring spatially heterogeneous pathological images. However, there have been very few, if any, studies that have systematically evaluated the current Transformer-based approaches in pathological image segmentation. To assess the performance of Transformer segmentation models on whole slide images (WSI), we quantitatively evaluated six prevalent transformer-based models on tumor segmentation, using the widely used PAIP liver histopathological dataset. For a more comprehensive analysis, we also compare the transformer-based models with six major traditional CNN-based models. The results show that the Transformer-based models exhibit a general superior performance over the CNN-based models. In particular, Segmenter, Swin-Transformer and TransUNet-all transformer-based-came out as the best performers among the twelve evaluated models.

Keywords: liver tumor segmentation, semantic segmentation, histopathological image analysis, Transformer

1. INTRODUCTION

Digital pathological image analysis where diseased tissues are examined under WSI leads to a paradigm shift in clinical practice that allows the pathologists to assess the digitized tissues remotely. Moreover, computer-aided methods can be deployed on the digital WSI to further assist and practically automate the quantification of cancer tissues for histopathologists, which is currently a tedious and resource-intensive process.¹The past few years had witnessed a tremendous success of deep learning in digital pathology. In particular, researchers have developed and deployed a convolutional neural network (CNN) with the encoder-decoder architecture to segment tumor tissues. Notable approaches include U-Net,² DeepLabV3,³ PAN,⁴ etc. Limited by the nature of the local convolution operations, CNNs tend to focus on local details in segmentation, without capturing the global information.^{5,6} Recently, Transformers have emerged as a new deep learning paradigm for semantic segmentation. Moreover, recent studies have shown that the Transformers can achieve superior performance as compared with the CNN-based approaches in various semantic segmentation applications.⁷⁻¹³ The major advantage of Transformers over CNN is their superior ability in capturing the global contextual information of an image, including long-distance relationships and dependencies. The state-of-the-art Transformer-based semantic segmentation methods can be roughly ascribed to two categories: (1) convolution-free design^{9,12,13} and (2) CNN-Transformer hybrid design.^{10,11} Besides this, the Transformer can be used as a pre-training tool to learn a representation model for the downstream semantic segmentation.⁸

Even with promising results in a variety of semantic segmentation tasks, there are very few, if any, existing studies that systematically evaluate the Transformers for histopathological image segmentation. In this paper, we provide a quantitative performance evaluation of six recent transformer models and compare them with six traditional CNN-based methods (total of 12 segmentation methods)-for tumor segmentation using the liver histopathological images (Table.1).

Corresponding author: Yuankai Huo: E-mail: yuankai.huo@vanderbilt.edu

Transformer-Based Models	Acronym	Year	Download URL
TransUNet ¹⁰	TUNet	2021	https://github.com/Beckschen/TransUNet
Swin-Unet ⁹	SUNet	2021	https://github.com/HuCaoFighting/Swin-Unet
Swin-Transformer ¹³	Swin-Trans	2021	https://github.com/SwinTransformer/Swin-Transformer-Object-Detection
Segmenter ¹²	Segm	2021	https://github.com/rstrudel/segmenter
Medical-Transformer ¹¹	MedT	2021	https://github.com/jeya-maria-jose/Medical-Transformer
BERT Image Transformers ⁸	BEiT	2021	https://github.com/microsoft/unilm/tree/master/beit
CNN-Based Models			
Pyramid Scene Parsing Net ¹⁴	PSPNet	2016	https://pypi.org/project/segmentation-models-pytorch/
U-Net ²	U-Net	2015	https://pypi.org/project/segmentation-models-pytorch/
DeepLabV3 ³	DLV3	2016	https://pypi.org/project/segmentation-models-pytorch/
Feature Pyramid Network ¹⁵	FPN	2016	https://pypi.org/project/segmentation-models-pytorch/
Pyramid Attention Network ⁴	PAN	2018	https://pypi.org/project/segmentation-models-pytorch/
LinkNet ¹⁶	LinkNet	2018	https://pypi.org/project/segmentation-models-pytorch/

Table 1. This table lists the six CNN methods and six Transformer methods that are evaluated in this study.

2. METHOD

2.1 Overall Framework

Fig.1 shows the overall semantic segmentation pipeline for different approaches. To perform the semantic segmentation networks (SSN) on a Gigapixel histopathological image, the entire WSI is tiled into smaller patches at either $20\times$ or $40\times$ with the same patch size 512×512 . During the training stage, the patch sampler randomly crops training patches from the PAIP liver tumor dataset.¹⁷ Since a WSI usually has large non-tissue areas that can be excluded from the computation, we discard patches in which more than half of the areas are background (i.e those with RGB values between 240-255).

During the testing stage, to enable more smoothed global segmentation results, we allow for an overlap of neighboring patches, which is set to half of the patch size in both the horizontal and vertical directions. Each image patch is then fed into an SSN in order to achieve a predicted tumor segmentation mask. All image patches that belong to the same WSI are fused to a global segmentation mask with the same size as the original WSI. The performance of an SSN algorithm is evaluated by comparing the final global segmentation mask and the provided ground truth mask. For this purpose, we use the Jaccard index (also known as the IOU¹⁸), which is the ratio of the intersection of the predicted and ground truth masks to their union.

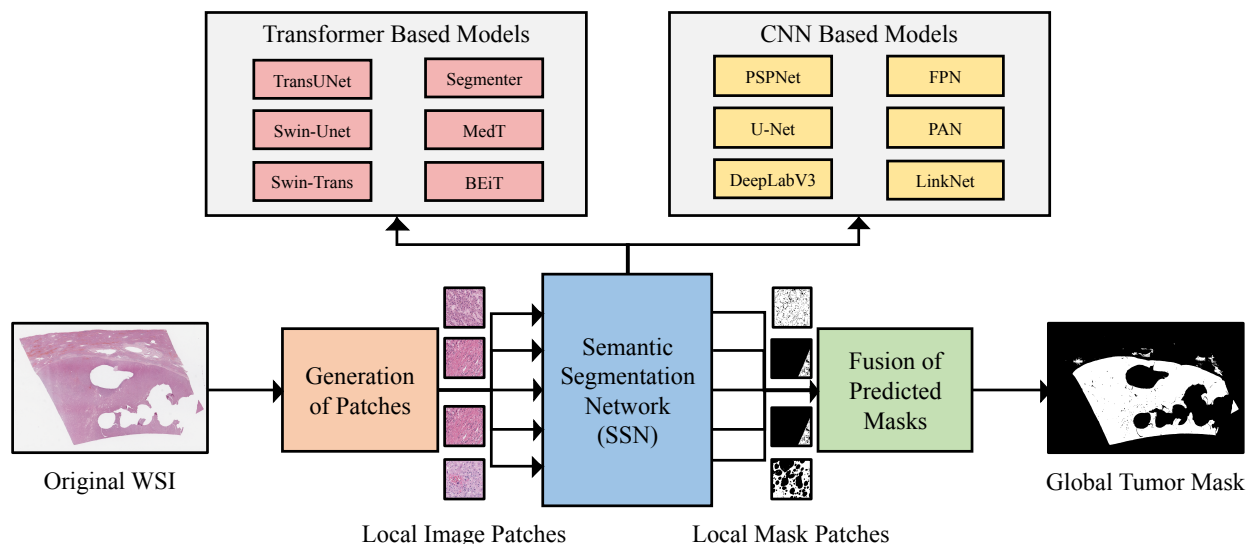


Figure 1. A pipeline of both CNN-based and Transformer-based cancer diagnosis

2.2 Transformer based Methods

Six transformer-based SSN models, whose open-source code is available, are employed in this study:

1. **TransUNet:**¹⁰ This model combines a Transformer with a CNN while still using the U-Net architecture. Specifically, they proposed a CNN-Transformer Hybrid Encoder. The transformers use the feature map, created by the CNN, as an input instead of a raw image. They also used a cascaded up-sampler as their decoder. In our experiment, we used R50-ViT-B_16 which is a hybrid of ResNet-50 and ViT.⁷
2. **Swin-Unet:**⁹ Unlike TransUNet, Swin-Unet is a purely transformer-based model with the encoder decoder architecture of U-Net. Like U-Net, this model has skip connections for local features. We used the initial checkpoint provided.
3. **Swin-Transformer:**¹³ This model is a hierarchical Transformer that can serve as a general backbone for various computer vision tasks. The representation is computed with shifted windows limiting self-attention computation to non-overlapping local windows. This makes the model efficient and flexible, also making it usable on image classification, object detection, and semantic segmentation. This is also a pure transformer. The open source code provides three configurations: tiny, small, and base. We report here the results of the tiny model.
4. **Segmenter:**¹² This is a fully transformer-based model. The encoder is made up of Multi-head Self Attention (MSA) blocks and Multi-Layer Perceptron blocks, as well as two layer norms before each block and residual connections after each block. Segmenter uses a linear decoder bilinearly up-sampling the sequence into a 2D segmentation mask. The source code provides three models: small, base, and large. We report here the results of the base model.
5. **Medical Transformer:**¹¹ This model builds upon a basic Transformer-Based architecture with gated axial-attention blocks. The axial-attention blocks are composed of two self-attention blocks: one focusing on the width and the other focusing on the height. They are able to control the influence of the learned positional encodings on encoding non-local context.
6. **BEiT:**⁸ This method uses a transformer to learn a representation model through self-supervision training on ImageNet. They then use this representation as a backbone encoder and incorporate several deconvolution layers as a decoder to produce segmentation. In this experiment, we used the BEiT base model that was pretrained on ImageNet22K.

To train these networks we used their provided open-source codes and fed them with data from our patch sampler. In each round of training, we fed 128 random examples to the network. These examples were randomly cropped from WSIs at a given level (40 magnification or 20 magnification) and put into batches of 8. Each model was trained for 1000 rounds. After each round, we computed the average loss of the model on the validation set. The model with the lowest loss value was retained and evaluated on the full set of the test slides using the Jaccard index. To eliminate the sensitivity to the learning rate, we trained each aforementioned model with different initial learning rates (0.01, 0.001, 0.0001) and only the best result is reported based on the validation set.

2.3 CNN based methods

We also compared the above algorithms with major CNN-based semantic segmentation models including PSP-Net,¹⁴ U-Net,² DeepLabV3,³ FPN,¹⁵ PAN,⁴ and LinkNet.¹⁶ These models were implemented using the open-source Semantic Segmentation Models package.¹⁹

3. DATASET AND EXPERIMENTS

We employed the PAIP Grand Challenge dataset¹⁷ to evaluate our histopathological image analysis algorithms. In this challenge, the participants had access to 100 WSIs of the liver collected by Seoul National University Hospital. Only 50 of them had ground truth segmentation masks publicly available as the other 50 were used for validation. Each image contains only a single tumor lesion from each patient. PAIP provides two types of

CNN-based Models	40× Magnification	20× Magnification
PSPNet ¹⁴	0.58 ± 0.33	0.49 ± 0.27
U-Net ²	0.65 ± 0.24	0.60 ± 0.31
DeepLabV3 ³	0.63 ± 0.28	0.67 ± 0.24
FPN ¹⁵	0.64 ± 0.20	0.72 ± 0.22
PAN ⁴	0.63 ± 0.24	0.69 ± 0.23
LinkNet ¹⁶	0.35 ± 0.33	0.54 ± 0.25
Tranformer-Based Models	40× Magnification	20× Magnification
TransUNet(R50-ViT-B_16) ¹⁰	0.77 ± 0.12	0.77 ± 0.13
Swin-Unet ⁹	0.53 ± 0.23	0.42 ± 0.23
Swin-Transformer(base) ¹³	0.79 ± 0.14	0.71 ± 0.26
Segmenter ¹²	0.80 ± 0.14	0.82 ± 0.11
Medical Transformer ¹¹	0.71 ± 0.14	0.62 ± 0.17
BEiT ⁸	0.72 ± 0.21	0.66 ± 0.28

Table 2. Average Jaccard index for viable tumors with a patch size of 512

tumor masks: viable and whole. The viable tumor is defined as the region containing the cell nest and the active cancerous parts of the tumor while the whole tumor contains the cell nests as well as the dead tissue surrounding the viable tumor and the tumor capsules. The results in this paper were obtained for the viable tumor type only. The slides were H&E dyed, scanned by Aperio AT2 at ×20 power, and compressed into SVS format with the average size of 80,000×80,000 pixels. We only used the 50 slides with ground truth in this work. Furthermore, we used 40 of those slides for training the SSN models while the remaining 10 were used for the testing. We also used a small validation set for selecting the best model during training. It consists of 150 patches randomly cropped from the test slides.

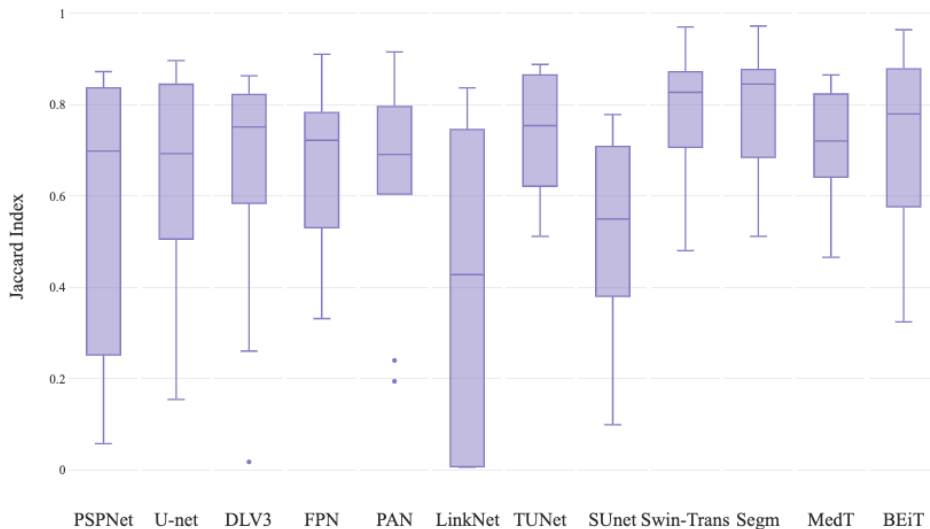


Figure 2. Tumor segmentation performance of different SSNs for patch size 512 and 40× magnification

4. RESULTS

The results are shown for the selected models in Table 2 for the segmentation of viable tumors at the pyramid levels: 40× magnification and 20× magnification. The reported Jaccard index is averaged over all ten test slides. The chart in Fig.2 shows the average Jaccard index for different pyramid levels. Fig.3 shows the predicted tumor mask for some test slides along with their ground truth.

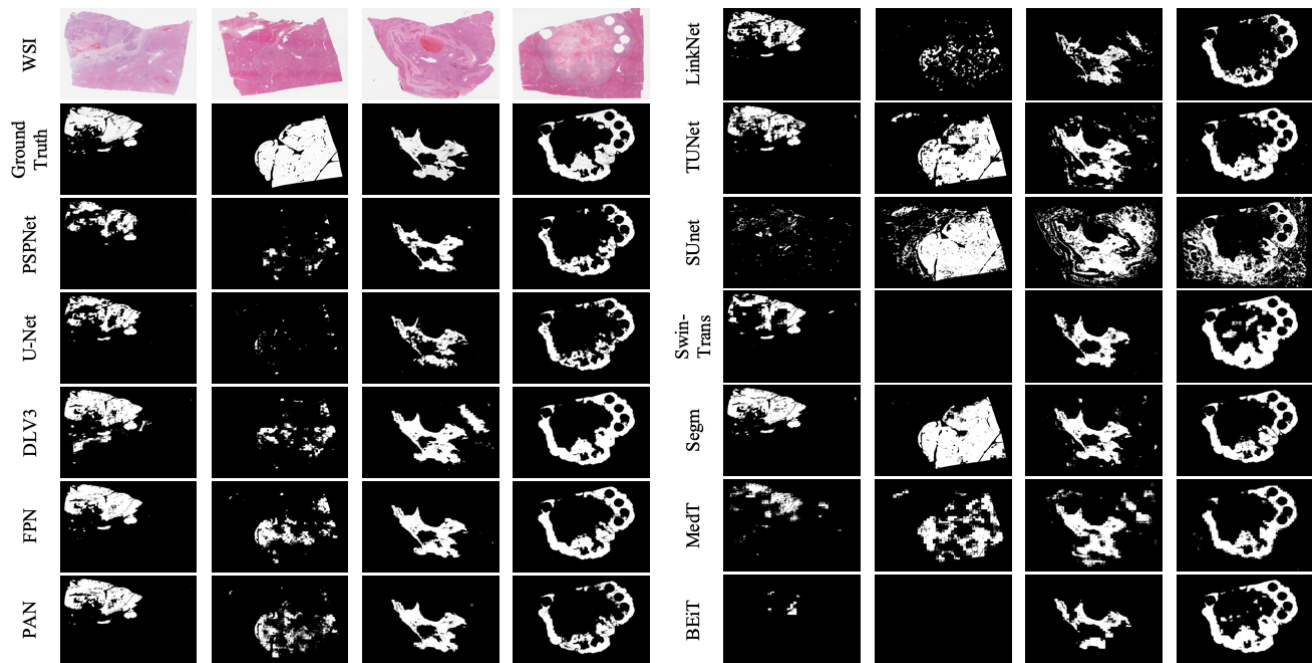


Figure 3. This figure presents the qualitative segmentation results using different approaches.

Several remarks can be made from the results:

1. Transformer-based models tend to outperform FCN with the exception of Swin-Unet. This is consistent with published results in other application domains.
2. Our best average Jaccard index value 0.82 was obtained with Segmenter at patch size 512 magnification. Segmenter also achieved the highest scores at both resolution levels.
3. As shown by the results, Segmenter, Swin-Transformer, and TransUNet are the best performers. Both Segmenter and TransUNet are built upon the vision transformer ViT,⁷ while Swin-Transformer is a hierarchical version of it. These three models were pretrained on ImageNet while other models such as Medical Transformer and BEiT were not. This could be a possible explanation for their superior performance.
4. While both Segmenter and Swin-Unet are fully transformer-based, Segmenter is the best model while Swin-Unet is the worst. Therefore, the performance most likely does not depend on whether the model is fully transformer-based or hybrid.

5. DISCUSSION

We have implemented an image analysis pipeline for tumor segmentation in whole-slide images. Using this pipeline we could evaluate the performance of different semantic segmentation models on a fair bases. Specifically, we quantitatively evaluated six state-of-the-art transformer-based models on the PAIP dataset and compared them with six major traditional CNN-based methods. The results showed that several transformer-based models indeed exhibit superior performance over the CNN-based models. In particular, Segmenter,¹² Swin-Transformer¹³ and TransUNet¹⁰-all transformer-based-came out as the best performances among the twelve evaluated models.

6. ACKNOWLEDGMENTS

This work has not been submitted for publication or presentation elsewhere.

REFERENCES

- [1] He, L., Long, L. R., Antani, S., and Thoma, G. R., “Histology image analysis for carcinoma detection and grading,” *Computer Methods and Programs in Biomedicine* **107**(3), 538–556 (2012).
- [2] Ronneberger, O., Fischer, P., and Brox, T., “U-net: Convolutional networks for biomedical image segmentation,” in [*International Conference on Medical image computing and computer-assisted intervention*], 234–241, Springer (2015).
- [3] Chen, L., Papandreou, G., Kokkinos, I., Murphy, K., and Yuille, A. L., “Deeplab: Semantic image segmentation with deep convolutional nets, atrous convolution, and fully connected crfs,” *IEEE Transactions on Pattern Analysis and Machine Intelligence* **40**(4), 834–848 (2018).
- [4] Li, H., Xiong, P., An, J., and Wang, L., “Pyramid attention network for semantic segmentation,” *CoRR* **abs/1805.10180** (2018).
- [5] Huo, Y., Deng, R., Liu, Q., Fogo, A. B., and Yang, H., “Ai applications in renal pathology,” *Kidney international* (2021).
- [6] Liu, Q., Louis, P. C., Lu, Y., Jha, A., Zhao, M., Deng, R., Yao, T., Roland, J. T., Yang, H., Zhao, S., et al., “Simtriplet: Simple triplet representation learning with a single gpu,” *arXiv preprint arXiv:2103.05585* (2021).
- [7] Dosovitskiy, A., Beyer, L., Kolesnikov, A., Weissenborn, D., Zhai, X., Unterthiner, T., Dehghani, M., Minderer, M., Heigold, G., Gelly, S., Uszkoreit, J., and Houlsby, N., “An image is worth 16x16 words: Transformers for image recognition at scale,” *CoRR* **abs/2010.11929** (2020).
- [8] Bao, H., Dong, L., and Wei, F., “Beit: BERT pre-training of image transformers,” *CoRR* **abs/2106.08254** (2021).
- [9] Cao, H., Wang, Y., Chen, J., Jiang, D., Zhang, X., Tian, Q., and Wang, M., “Swin-unet: Unet-like pure transformer for medical image segmentation,” (2021).
- [10] Chen, J., Lu, Y., Yu, Q., Luo, X., Adeli, E., Wang, Y., Lu, L., Yuille, A. L., and Zhou, Y., “Transunet: Transformers make strong encoders for medical image segmentation,” *CoRR* **abs/2102.04306** (2021).
- [11] Valanarasu, J. M. J., Oza, P., Hacihaliloglu, I., and Patel, V. M., “Medical transformer: Gated axial-attention for medical image segmentation,” *CoRR* **abs/2102.10662** (2021).
- [12] Strudel, R. A. M., Garcia, R., Laptev, I., and Schmid, C., “Segmenter: Transformer for semantic segmentation,” *CoRR* **abs/2105.05633** (2021).
- [13] Liu, Z., Lin, Y., Cao, Y., Hu, H., Wei, Y., Zhang, Z., Lin, S., and Guo, B., “Swin transformer: Hierarchical vision transformer using shifted windows,” *CoRR* **abs/2103.14030** (2021).
- [14] Zhao, H., Shi, J., Qi, X., Wang, X., and Jia, J., “Pyramid scene parsing network,” in [*Proceedings of the IEEE conference on computer vision and pattern recognition*], 2881–2890 (2017).
- [15] Lin, T., Dollár, P., Girshick, R. B., He, K., Hariharan, B., and Belongie, S. J., “Feature pyramid networks for object detection,” *CoRR* **abs/1612.03144** (2016).
- [16] Chaurasia, A. and Culurciello, E., “Linknet: Exploiting encoder representations for efficient semantic segmentation,” in [*2017 IEEE Visual Communications and Image Processing (VCIP)*], 1–4 (2017).
- [17] “Paip 2019 - grand challenge.” <https://paip2019.grand-challenge.org/>.
- [18] Wikipedia contributors, “Jaccard index — Wikipedia, the free encyclopedia.” https://en.wikipedia.org/w/index.php?title=Jaccard_index&oldid=977019056 (2020). [Online; accessed 14-November-2020].
- [19] Yakubovskiy, P., “segmentation-models-pytorch.” <https://pypi.org/project/segmentation-models-pytorch/> (2020).